Pergamon

Int. J. Solids Structures Vol. 33, No. 12, pp. 1673–1688, 1996

0020-7683/96 $15.00 + .00

0020-7683(95)00128-X

DYNAMIC FINITE ELEMENT ANALYSIS OF A NONLINEAR BEAM SUBJECTED TO A MOVING LOAD

T.-P. CHANG and Y.-N. LIU
Department of Applied Mathematics, National Chung-Hsing University, Taichung, Taiwan, Republic of China

(*Received* 2 *November* 1994; *in revised form* 26 *May* 1995)

Abstract—In this paper, the deterministic and random vibration analysis of a nonlinear beam on an elastic foundation subjected to a moving load, which may simulate railway track, runway, etc. has been performed. The effects of longitudinal deflection and inertia have been considered so that the coupled equations of longitudinal and transverse deflections can be derived based on Bernoulli–Euler hypothesis. The randomness of the beam profile has been considered in such a way that the mean line of the beam is variable with respect to position in the vertical plane and is superimposed by stochastic uncertainty, and the moving load travels along the beam with constant velocity or acceleration. The deterministic and statistical dynamic responses of the beam have been calculated by using the Galerkin's method in conjunction with the finite element method, and the derived nonlinear system differential equation has been solved by using the implicit direct integration method. In particular, the standard deviation of the transverse deflection of the nonlinear beam has been calculated and presented by using the Monte Carlo simulation technique. Also, the distribution of the midpoint deflection of the beam has been investigated by using the probability paper plot.

1. INTRODUCTION

The nonlinear vibration analysis of a beam has been performed by several researchers. Mei (1972) studied the nonlinear vibration of the beams using the matrix displacement method. Raju *et al.* (1976) adopted the Galerkin method with finite element method to investigate the large amplitude-free vibration of tapered beams. Prathap and Bhashyam (1980) also used the same method to study the nonlinear vibration of beams. Sato (1980) analyzed the nonlinear vibrations of stepped thickness beams by the transfer matrix method. Hino *et al.* (1984, 1985) studied the nonlinear vibrations of variable cross-sectional beams subjected to a moving load by using the Galerkin method with finite element method. Suzuki (1977) investigated the dynamic behaviour of a finite beam subjected to a traveling load with acceleration. However, all these papers were limited to the case where the loading condition and the beam was analyzed deterministically. Fryba (1976) studied the nonstationary response of a beam subjected to a moving random load. Yoshimura *et al.* (1988) used the finite element method to perform the random vibration analysis of a nonlinear beam with variable sectional areas subjected to a moving load.

The purpose of this paper is to perform the deterministic and random vibration analysis of a nonlinear beam on an elastic foundation subjected to a moving load. The effects of longitudinal deflections and inertia have been considered so that the coupled equations of longitudinal and transverse deflections can be derived based on Bernoulli–Euler hypothesis. The randomness of the beam profile has been considered in such a way that the mean line of the beam is variable with respect to position in the vertical plane and is superimposed by stochastic uncertainty, and the moving load travels along the beam with constant velocity or acceleration. It should be noted that the above assumption will introduce the nonstationarity to the whole system. The deterministic and statistical dynamic responses of the beam have been calculated by using Galerkin method in conjunction with the finite element method, and the nonlinear system differential equation has been solved by using the implicit direct integration method. In particular, the standard deviation of the transverse deflection of the nonlinear beam has been calculated and presented by using the Monte

Carlo simulation technique. Besides, the distribution of the midpoint deflection of the beam has been investigated by using the propability paper plot.

2. STATEMENT OF THE PROBLEM

2.1. *System model*

The stochastic beam on an elastic foundation is used to simulate train (or vehicle), track and the foundation (Fig. 1). The rail–wheel contact is assumed to be at one point only, the vehicle suspension system is idealized to consist of one linear spring and one viscous damper, and the vehicle is modeled as a lumped mass.

The track is assumed to be a finite length slender beam of uniform cross-section and density. The track mean line is variable in the vertical plane and is superimposed by random unevenness. The vertical track profile, measured from a flat datum, may be expressed in terms of x, the distance along the track, as

$$h(x) = h_{\mathrm{m}}(x) + h_{\mathrm{R}}(x) = h_{\mathrm{m}}(x) + \int_{-\infty}^{\infty} \mathrm{e}^{-j\Omega x}\, \mathrm{d}Q(\Omega), \quad j = \sqrt{-1}, \tag{1}$$

where $h_{\mathrm{m}}(x)$ is a deterministic function representing the track mean, $h_{\mathrm{R}}(x)$ is zero mean

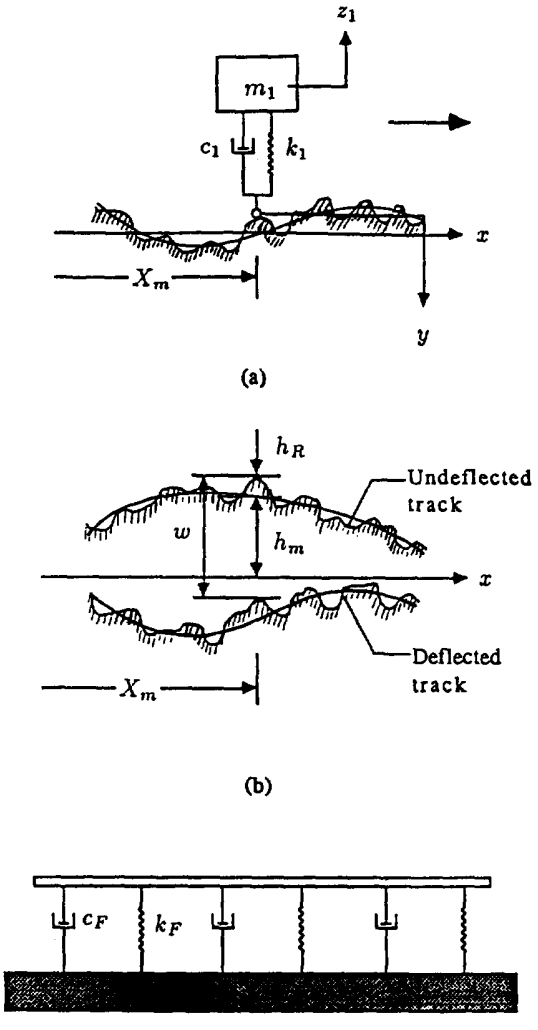

Fig. 1. System model. (a) Vehicle model; (b) track profile and deflection; (c) track and foundation model.

random process, Ω is the spatial frequency, and $Q(\Omega)$ is an orthogonal function with the properties

$$\mathbf{E}[|\mathrm{d}Q(\Omega)|] = \mu_{h_R}\,\mathrm{d}\Omega = 0, \mathbf{E}[|\mathrm{d}Q(\Omega_1)\,\mathrm{d}Q^*(\Omega_2)|] = S_{h_R}(\Omega_1,\Omega_2)\delta(\Omega_1-\Omega_2)\,\mathrm{d}\Omega_1\,\mathrm{d}\Omega_2, \tag{2}$$

where $\mathbf{E}(\bullet)$ denotes the expectation, μ_{h_R} is the mean value of $h_R(x)$, S_{h_R} is the power spectral density function of $h_R(x)$, $\delta(\bullet)$ denotes the Dirac Delta function and the asterisk denotes the complex conjugate.

The second derivative process of the track profile with respect to x should exist. The form for the mean adopted in the present study is

$$h_m(x) = \sum_{i=1}^{n_1} h_i \sin 2\pi x/L_i, \tag{3}$$

here h_i and L_i are constants, which are selected to represent various mean shapes. Nevertheless any other acceptable expression can be used for the mean profile.

It is proposed to assume the homogeneous track power spectrum density as

$$S_{h_R}(\Omega) = A_1 \exp(-\Omega^2/a^2), \tag{4}$$

where A_1 and a are constants for a particular class of track.

In general, the train moves along the ground with variable velocity. Its position along the track X_m at any instant t may be modeled as a polynomial in t. The form adopted in generating the results is

$$X_m(t) = b_0 + b_1 t + b_2 t^b, \tag{5}$$

b_0, b_1, b_2 and b are constants selected to fit a motion train. Any other form considered appropriate for train ground motion description can be used in place of eqn (5).

2.2. *System equation*

Again for Fig. 1, when the rotary inertia, shearing deformations and out-of-plane motion for the track are neglected, the governing differential equations for the nonlinear transverse and longitudinal deflections of the track, w, u, and for the deflections vertical to the moving direction of the train, z_1, are, respectively, as follows

$$\rho_T A_T \frac{\partial^2 u}{\partial t^2} - \frac{\partial}{\partial x}\left\{EA_T\left[\frac{\partial u}{\partial x} + \frac{1}{2}\left(\frac{\partial w}{\partial x}\right)^2\right]\right\} = 0, \tag{6}$$

$$EI\frac{\partial^4 w}{\partial x^4} + \rho_T A_T \frac{\partial^2 w}{\partial t^2} - \frac{\partial}{\partial x}\left\{EA_T\left[\frac{\partial u}{\partial x} + \frac{1}{2}\left(\frac{\partial w}{\partial x}\right)^2\right]\frac{\partial w}{\partial x}\right\} = f(x,t) - s(x,t), \tag{7}$$

$$m_1\ddot{z}_1 + c_1(\dot{z}_1 + \dot{w}) + k_1(z_1 + w - h) = 0, \tag{8}$$

where ρ_T and A_T are the density and cross-section of the track, respectively, and E is Young's modulus, I the area moment of inertia, $f(x,t)$ the impressed force on the track and $s(x,t)$ the restoring force distribution imposed by the foundation, h is the vertical track profile, c_1 and k_1 are the damping and stiffness coefficients of the vehicle suspension system.

For the single-point rail–wheel contact

$$f(x,t) = -[c_1(\dot{z}_1+\dot{w})+k_1(z_1+w-h)]\delta(x-X_m), \tag{9}$$

where $\delta(\cdot)$ denotes Dirac Delta function.

The foundation reaction is given by

$$s(x,t) = k_F w + c_F\frac{\partial w}{\partial t} + \rho_F A_F\frac{\partial^2 w}{\partial t^2}, \tag{10}$$

where ρ_F is the foundation density, A_F is the effective cross-section of the foundation, and k_F and c_F are the effective foundation stiffness and damping coefficients per unit length. The first term denotes the elastic force, the second the damping effect, and the third the inertial contribution of the vibrating foundation.

Substitution of eqns (9) and (10) into eqn (7) yields

$$EI\frac{\partial^4 w}{\partial x^4}+\rho\frac{\partial^2 w}{\partial t^2}+c_F\frac{\partial w}{\partial t}+k_F w-\frac{\partial}{\partial x}\left\{EA_T\left[\frac{\partial u}{\partial x}+\frac{1}{2}\left(\frac{\partial w}{\partial x}\right)^2\right]\frac{\partial w}{\partial x}\right\}$$
$$= -[c_1(\dot{z}_1+\dot{w})+k_1(z_1+w-h)]\delta(x-X_m), \tag{11}$$

where $\rho = \rho_F A_F + \rho_T A_T$.

The boundary conditions for the simply supported track of length L are

$$u = 0, \quad w = 0, \quad EI\left(\frac{\partial^2 w}{\partial x^2}\right) = 0 \quad \text{at } x = 0 \quad \text{and} \quad L$$

and the initial conditions for the track and the moving train at $t = 0$ are, respectively,

$$u = u_0(x), \quad \frac{\partial u}{\partial t} = \dot{u}_0(x), \quad w = w_0(x), \quad \frac{\partial w}{\partial t} = \dot{w}_0(x), \quad z_1 = z_{1_0}, \quad \frac{dz_1}{dt} = \dot{z}_{1_0}.$$

2.3. *Finite element formulation*

The finite element formulation is generally effective for obtaining approximate solutions for complicated problems with high accuracy. Here, a Galerkin's finite element formulation is used.

Assume $\bar{u}(x,t)$ and $\bar{w}(x,t)$ are the approximate solutions of $u(x,t)$ and $w(x,t)$, respectively, and

$$\bar{u}(x,t) = \sum_{i=1}^{m} S_i(x)\psi_i(t) = [S]\{\psi\} \tag{12}$$

$$\bar{w}(x,t) = \sum_{i=1}^{n} N_i(x)\phi_i(t) = [N]\{\phi\} \tag{13}$$

where the S_is and N_is are shape functions in an element, the ψ_is and ϕ_is are unknown time functions of nodal values, and m and n denote the number of nodes in the element. When eqns (12) and (13) are substituted into eqn (6), the residual ε_a is defined as the difference between the approximate and the exact solutions, the residual ε_t is similarly defined for eqn (11). Galerkin's method distributes the residuals over the element among the weighting functions (S_is or N_is) such that

$$\int_{D_a} S_i \varepsilon_a \, \mathrm{d}D_a = 0, \quad i = 1, 2, \ldots, m, \tag{14}$$

$$\int_{D_t} N_i \varepsilon_t \, \mathrm{d}D_t = 0, \quad i = 1, 2, \ldots, n, \tag{15}$$

i.e. the weighting functions S_i and N_i are orthogonal to the residual in the integral domains D_a and D_t, respectively.

The formulation for an optional element is as follows:

$$\int_0^H [S]^{\mathrm{T}} \left\{ \rho_{\mathrm{T}} A_{\mathrm{T}} \frac{\partial^2 \bar{u}}{\partial t^2} - \frac{\partial}{\partial x} \left\{ EA_{\mathrm{T}} \left[\frac{\partial \bar{u}}{\partial x} + \frac{1}{2} \left(\frac{\partial \bar{w}}{\partial x} \right)^2 \right] \right\} \right\} \mathrm{d}x = 0, \tag{16}$$

$$\int_0^H [N]^{\mathrm{T}} \left\{ EI \frac{\partial^4 \bar{w}}{\partial x^4} + \rho \frac{\partial^2 \bar{w}}{\partial t^2} + c_{\mathrm{F}} \frac{\partial \bar{w}}{\partial t} + k_{\mathrm{F}} \bar{w} - \frac{\partial}{\partial x} \left\{ EA_{\mathrm{T}} \left[\frac{\partial \bar{u}}{\partial x} + \frac{1}{2} \left(\frac{\partial \bar{w}}{\partial x} \right)^2 \right] \frac{\partial \bar{w}}{\partial x} \right\} - \bar{f}(x, t) \right\} \mathrm{d}x = 0, \tag{17}$$

where $\bar{f}(x, t) = -[c_1(\dot{z}_1 + \dot{\bar{w}}) + k_1(z_1 + \bar{w} - h)]\delta(x - X_{\mathrm{m}})$ and H is the length of an element, and T denotes matrix transposition. After partial integration has been applied to eqns (16) and (17), the equation for all the elements of the beam are assembled, with account of boundary conditions, and the finite element formulation in the spatial domain is then given by

$$[MA]\{\ddot{\psi}\} + [KA]\{\psi\} - \{PF\} = 0, \tag{18}$$

$$[MT]\{\ddot{\phi}\} + [CT]\{\dot{\phi}\} + [KT]\{\phi\} + c_1[N(x_b)]^{\mathrm{T}} \dot{z}_1 + k_1[N(x_b)]^{\mathrm{T}} z_1 - \{F\} = 0. \tag{19}$$

Here $[MA]$ is the axial mass matrix, $[KA]$ is the stiffness matrix, $\{PF\}$ is the axial force vector generated by transverse deflections, $[MT]$ is the transverse mass matrix, $[KT]$ is the stiffness matrix, $[CT]$ is the transverse damping matrix and $\{F\}$ is the load vector generated by the moving load. These matrices and vectors are defined as follows:

$$[MA] = \sum_{j=1}^{NE} \int_0^H [S]^{\mathrm{T}} \rho_{\mathrm{T}} A_{\mathrm{T}} [S] \, \mathrm{d}x,$$

$$[KA] = \sum_{j=1}^{NE} \int_0^H \frac{\mathrm{d}[S]^{\mathrm{T}}}{\mathrm{d}x} EA_{\mathrm{T}} \frac{\mathrm{d}[S]}{\mathrm{d}x} \mathrm{d}x,$$

$$\{PF\} = -\sum_{j=1}^{NE} \int_0^H \frac{\mathrm{d}[S]^{\mathrm{T}}}{\mathrm{d}x} EA_{\mathrm{T}} \left[\tfrac{1}{2} \{\phi\}^{\mathrm{T}} \frac{\mathrm{d}[N]^{\mathrm{T}}}{\mathrm{d}x} \frac{\mathrm{d}[N]}{\mathrm{d}x} \{\phi\} \right] \mathrm{d}x,$$

$$[MT] = \sum_{j=1}^{NE} \int_0^H [N]^{\mathrm{T}} \rho [N] \, \mathrm{d}x,$$

$$[CT] = [C] + [CP],$$

$$[C] = \sum_{j=1}^{NE} \int_0^H [N]^{\mathrm{T}} c_{\mathrm{F}} [N] \, \mathrm{d}x,$$

$$[CP] = \sum_{j=1}^{NE} \int_0^H [N]^{\mathrm{T}} c_1 [N] \delta(x - x_{\mathrm{m}}) \, \mathrm{d}x = \sum_{j=1}^{NE} [N(x_b)]^{\mathrm{T}} c_1 [N(x_b)],$$

$$[KT] = [KL] + [K] + [KG] + [KP],$$

$$[KL] = \sum_{j=1}^{NE} \int_0^H \frac{d^2[N]^T}{dx^2} EI \frac{d^2[N]}{dx^2} dx,$$

$$[K] = \sum_{j=1}^{NE} \int_0^H [N]^T k_F [N]\, dx,$$

$$[KG] = \sum_{j=1}^{NE} \int_0^H \frac{d[N]^T}{dx} \left\{ EA_T \left[\frac{d[S]}{dx} \{\psi\} + \tfrac{1}{2}\{\phi\}^T \frac{d[N]^T}{dx} \frac{d[N]}{dx} \{\phi\} \right] \right\} \frac{d[N]}{dx} dx,$$

$$[KP] = \sum_{j=1}^{NE} \int_0^H [N]^T k_1 [N] \delta(x - X_m)\, dx = \sum_{j=1}^{NE} [N(x_b)]^T k_1 [N(x_b)],$$

$$\{F\} = \sum_{j=1}^{NE} \int_0^H [N]^T k_1 h \delta(x - X_m)\, dx = \sum_{j=1}^{NE} [N(x_b)]^T k_1 h, \tag{20}$$

where NE is the total number of elements. When the moving train is located at a specified element, the vector $[N(x_b)]$ is defined as

$$[N(x_b)] = [N_1(x_b) \quad N_2(x_b) \quad N_3(x_b) \quad N_4(x_b)], \tag{21}$$

where $[N(x_b)]$ is an elemental vector, and x_b is defined as

$$x_b = X_m - H \,\mathrm{trunc}\,(X_m/H), \tag{22}$$

where trunc$(\cdot)$ denotes the integral part in the parenthesis. However, when the moving train is located at all other elements except the specified element, $[N(x_b)]$ is

$$[N(x_b)] = [0\,0\,0\,0]. \tag{23}$$

Substituting eqn (13) into eqn (8) gives the equation of motion for the moving train as

$$m_1 \ddot{z}_1 + c_1 \dot{z}_1 + c_1 [N(x_b)]\{\dot{\phi}\} + k_1 z_1 + k_1 [N(x_b)]\{\phi\} = k_1 h. \tag{24}$$

Combining eqns (19) and (24) gives

$$\begin{bmatrix} [MT] & 0 \\ 0 & m_1 \end{bmatrix} \begin{Bmatrix} \ddot{\phi} \\ \ddot{z}_1 \end{Bmatrix} + \begin{bmatrix} [CT] & c_1 [N(x_b)]^T \\ c_1 [N(x_b)] & c_1 \end{bmatrix} \begin{Bmatrix} \dot{\phi} \\ \dot{z}_1 \end{Bmatrix} + \begin{bmatrix} [KT] & k_1 [N(x_b)]^T \\ k_1 [N(x_b)] & k_1 \end{bmatrix} \begin{Bmatrix} \phi \\ z_1 \end{Bmatrix} = \begin{Bmatrix} \{F\} \\ k_1 h \end{Bmatrix}. \tag{25}$$

Therefore, eqns (18) and (25) give the formulation in the spatial domain.

3. SOLUTION OF SYSTEM EQUATION

3.1. *Linearized approximation by incremental form*

It is generally suitable for multi-dimensional systems for non-linear equations to be linearized by the incremental displacement method (Nickell, 1976). Equation (25) at time $t+\Delta t$ is expressed as

$$[M]^{t+\Delta t}\{\ddot{\Phi}\}+[C]^{t+\Delta t}\{\dot{\Phi}\}+\{R(^{t+\Delta t}\{\Phi\})\}=\,^{t+\Delta t}\{F\}, \tag{26}$$

where $\{\Phi\}=\{\phi,\ z_1\}^{\mathrm{T}}$, and $\{R\}$ is a vector of restoring forces that depends upon the displacement field.

If the vector $\{R\}$ is differentiable in the neighbourhood of all deformed shapes $\{\Phi\}$, then the expansion

$$\{R(^{t+\Delta t}\{\Phi\})\}=\{R(^{t}\{\Phi\})\}+\left(\frac{\partial\{R\}}{\partial\{\Phi\}}\right)\Big|_{\{\Phi\}=^{t}\{\Phi\}}\{\Delta\Phi\}+\frac{1}{2}\left(\frac{\partial^2\{R\}}{\partial\{\Phi\}^2}\right)\Big|_{\{\Phi\}=^{t}\{\Phi\}}\{\Delta\Phi\}^2+\ldots \tag{27}$$

is obtained, where $\{\Delta\Phi\}=\,^{t+\Delta t}\{\Phi\}-\,^{t}\{\Phi\}$ is the incremental displacement. Substituting eqn (27) into eqn (26), defining the tangent stiffness matrix as

$$^{t}[K]=\left.\frac{\partial\{R\}}{\partial\{\Phi\}}\right|_{\{\Phi\}=^{t}\{\Phi\}}, \tag{28}$$

and neglecting the higher-order terms beyond the second derivatives gives the linearized equation

$$[M]^{t+\Delta t}\{\ddot{\Phi}\}+[C]^{t+\Delta t}\{\dot{\Phi}\}+\,^{t}[K]\{\Delta\Phi\}=\,^{t+\Delta t}\{F\}-\{R(^{t}\{\Phi\})\}. \tag{29}$$

Equations (18) and (29) are solved at the same time by time integration operators.

3.2. *Transitional analysis*

The transitional responses of the derived systems are calculated by using the Newmark method (Bathe *et al.*, 1976). Before the incremental solution is carried out, the linear constant structure matrices (i.e. the linearized effective stiffness, linear stiffness, mass and damping matrices) and the load vectors are assembled. During the step-by-step solution, the linearized effective stiffness matrix is updated for the nonlinearities in the system.

The incremental equilibrium equations at time $t+\Delta t$ are

$$[M]^{t+\Delta t}\{\ddot{\Phi}\}+[C]^{t+\Delta t}\{\dot{\Phi}\}+\,^{t}[K]\{\Delta\Phi\}=\,^{t+\Delta t}\{F\}-\,^{t}\{R\}, \tag{30}$$

$$[MA]^{t+\Delta t}\{\ddot{\psi}\}+[KA]\{\Delta\psi\}=\,^{t+\Delta t}\{PF\}-[KA]^{t}\{\psi\}. \tag{31}$$

To improve the solution accuracy of the nonlinear eqn (30), it is necessary to carry out the equilibrium iteration in each time step. The equilibrium equation is obtained as

$$[M]^{t+\Delta t}\{\ddot{\Phi}\}^{(i)}+[C]^{t+\Delta t}\{\dot{\Phi}\}^{(i)}+\,^{t}[K]^{(i-1)}\{\delta\Phi\}^{(i)}=\,^{t+\Delta t}\{F\}-\,^{t+\Delta t}\{R\}^{(i-1)},\quad i=1,2,3,\ldots \tag{32}$$

where $^{t+\Delta t}\{\ddot{\Phi}\}^{(i)}$, $^{t+\Delta t}\{\dot{\Phi}\}^{(i)}$ and $^{t+\Delta t}\{\Phi\}^{(i)}=\,^{t+\Delta t}\{\Phi\}^{(i-1)}+\{\delta\Phi\}^{(i)}$ are the vectors of accelerations, velocities and deflections at the ith iteration, respectively. The iterative computation is continued until

$$\frac{\|\{\delta\Phi\}^{(i)}\|}{\|^{t+\Delta t}\{\Phi\}^{(i)}\|}\leqslant \text{tol.} \tag{33}$$

is satisfied, where tol. denotes the tolerance and $\|\bullet\|$ denotes the Euclidean norm. Once the transverse deflection at time $t+\Delta t$, $^{t+\Delta t}\{\Phi\}$, is known, $^{t+\Delta t}\{PF\}$ can be calculated. As

${}^{t+\Delta t}\{PF\}$ is regarded as the axial force, the longitudinal deflections, velocities and accelerations, which correspond to ${}^{t+\Delta t}\{\psi\}$, ${}^{t+\Delta t}\{\dot{\psi}\}$ and ${}^{t+\Delta t}\{\ddot{\psi}\}$, respectively, at time $t+\Delta t$ are obtained.

4. MONTE CARLO SIMULATION AND PROBABILITY PAPER

In this study, Monte Carlo simulation method is used to perform the statistical dynamic analysis of the stochastic beam on the elastic foundation due to the complicated nature of the present problem. In order to generate many different sample functions to describe the fluctuation of the track, the random variable $h_R(x)$ in eqn (1) can be generated by using the following equation:

$$h_R(x) = \sqrt{2}\sum_{k=1}^{N} A_k \cos(\Omega_k x - \varphi_k), \tag{34}$$

where

$$A_k = \sqrt{S_{h_R}(\Omega_k)\Delta\Omega}, \tag{35}$$

$$\Omega_k = \Omega_l + (k-\tfrac{1}{2})\Delta\Omega, \tag{36}$$

$$\Delta\Omega = \frac{(\Omega_u - \Omega_l)}{N}, \tag{37}$$

where $S_{h_R}(\Omega_k)$ is the one sided spectral density of the random variable h_R, Ω_u is the upper cutoff wave number of the spectral density, Ω_l is the lower cutoff wave number of the spectral density, N is the total number of intervals in the discretization of the spectrum and φ_k is an independent random phase angle uniformly distributed between 0 and 2π.

Using eqn (34), a large number, say N_s, of sample functions of the stochastic field $h_R(x)$ can be generated, then different sample functions will produce different shapes of track. Combining with the deterministic part of track $h_m(x)$ in eqn (1), the whole vertical track profiles $h(x)$ for different samples are obtained, and the corresponding different load vectors in eqn (24) can be easily constructed.

Since we have simulated the unevenness track profile, the dynamic track problem is solved with aid of the Newmark integration algorithm N_s times for different sample functions of the stochastic functions field $h_R(x)$. Based on all these different dynamic responses, the statistical dynamic responses can be computed readily.

In the previous paragraph, we have discussed how to compute the statistical properties of deflection. However, it is interesting to know what distribution of deflection is. There are some methods which can accomplish the above task. In this paper, the probability paper is adopted for determining the distribution of the dynamic response. The concept of the probability paper is that a distribution function is represented by a straight line on its associated probability paper. That is, if the distribution function associated with the probability paper is really the population distribution function from which the random processes are taken, then it is expected that these points are scattered around a straight line within a reasonable small deviation. Hence, the distribution function associated with probability paper is accepted as the population distribution unless those points are evidently scattered around a curved line instead of a straight line.

5. NUMERICAL EXAMPLES AND DISCUSSIONS

In the present numerical calculations, the shape functions used in eqns (12) and (13) are, respectively, given by

$$S_1 = 1 - \frac{x}{H}, \tag{38}$$

$$S_2 = \frac{x}{H},$$

$$N_1 = 1 - \frac{3x^2}{H^2} + \frac{2x^3}{H^3},$$

$$N_2 = x - \frac{2x^2}{H} + \frac{x^3}{H^2},$$

$$N_3 = \frac{3x^2}{H^2} - \frac{2x^3}{H^3},$$

$$N_4 = -\frac{x^2}{H} + \frac{x^3}{H^2}. \tag{39}$$

The initial conditions for the longitudinal and transverse deflections of the beam and vertical deflections of the moving vehicle are assumed to be

$$u_0(x) = \dot{u}_0(x) = 0, w_0(x) = \dot{w}_0(x) = 0, z_{1_0} = \dot{z}_{1_0} = 0. \tag{40}$$

Nonlinear vibrations of the beam have been calculated for the following models:
Model 1: the longitudinal deflections and inertia are considered;
Model 2: the longitudinal deflections are considered, but the longitudinal inertia is not considered; i.e.

$$\rho_T A_T \left(\frac{\partial^2 u}{\partial t^2}\right) = 0; \tag{41}$$

and then

$$EA_T \left[\frac{\partial u}{\partial x} + \frac{1}{2}\left(\frac{\partial w}{\partial x}\right)^2\right] = \text{constant}; \tag{42}$$

Model 3: the longitudinal effects are not considered, i.e.

$$\rho_T A_T \left(\frac{\partial^2 u}{\partial t^2}\right) = 0; \tag{43}$$

and

$$\frac{\partial u}{\partial x} = 0. \tag{44}$$

The linear model is also performed in this study.

Numerical results have been generated with the following system parameter values: $L = 40.0$ ft(12.19 m), $E = 3.0 \times 10^4$ ksi(2.068×10^{11} Nm^{-2}), $I = 400.0$ in^4(1.66×10^{-4} m^4), $A_T = 0.5$ ft^2(0.046 m^2), $\rho_T = 15.2$ slug ft^{-3}(7840.2 kg/m^{-3}), $A_F = 5.0$ ft^2(0.465 m^2), $\rho_F = 5.0$ slug ft^{-3}(2579.0 kg/m^{-3}), $k_F = 1000.0$ lb ft^{-2} (47948.3 N m^{-2}), $m_1 = 40000.0$ slug(585454.6 kg), $k_1 = 40000.0$ lb ft^{-1} (584586.0 N m^{-1}), $\omega_1 = \sqrt{k_1/m_1} = 1.0$ rad sec^{-1}, $\zeta_1 = c_1/2m_1\omega_1 = 0.02$, $\omega_F = \sqrt{k_F/\rho} = 5.54$ rad sec^{-1}, $\zeta_F = c_F/2\rho\omega_F = 0.02$, $a = 1.0$ and

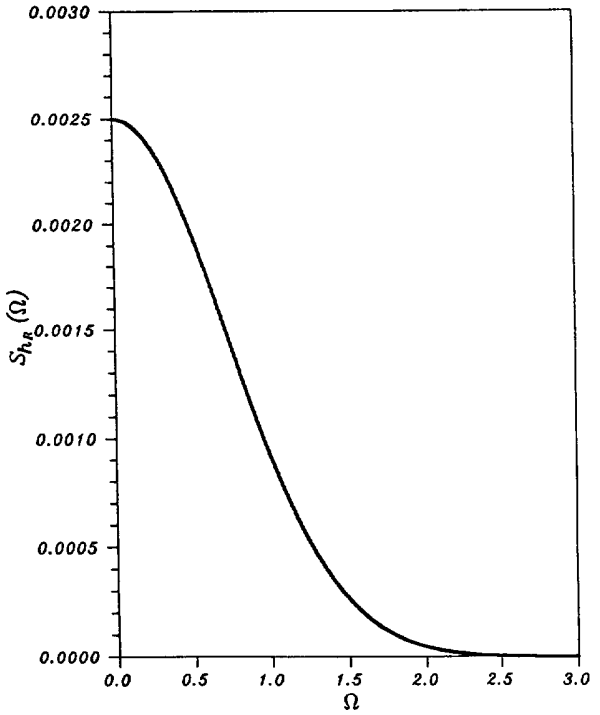

Fig. 2. Spectrum density of random variable $h_R(x)$.

$A_1 = 0.0025$ in^3 (4.10×10^{-8} m^3), where L is the length of the track, ω_1 and ω_F are the fundamental nature frequencies of the train and foundation, respectively, and ζ_1 and ζ_F are the damping ratios of the train and foundation, respectively. The total number of the finite element NE is 80, i.e. the length of each element H is equal to 0.5 ft. In order to perform Monte Carlo simulation, 100 different samples for the random variable h_R (x) were generated using the procedure mentioned previously. Figure 2 shows the assumed shape of the power spectral density function S_{h_R} of the track profile h_R, and six sample functions of the stochastic field h_R (x) are shown in Fig. 3.

Before the statistical analysis is performed, the deterministic analysis has been carried out in order to get a better understanding of the problem. It should be noted that the random variable $h_R(x)$ is equal to zero for the deterministic analysis. Figures 4–7 present the transverse deflection of the midpoint of the beam with respect to time due to various constant velocities and accelerations. It is understood that the beam will be in the state of free vibration when $X_m/L > 1.0$. It can be seen that the maximum deflection of the linear model is always greater than those of others, which is quite reasonable, besides, model 1 and model 2 have the same trend during the deflected processes. Also, it can be seen from Figs 4–7 that among those three nonlinear models, model 3 produced the largest maximum transverse deflection w, while model 1 produced the smallest maximum transverse deflection w.

The maximum deflections of the beam for various constant velocities for the four models are shown in Fig. 8. It should be noted that the beam is considered with the foundation and the mean profile of the track $h_m(x) = \sin 2\pi x/L$ ft. The maximum deflection increases as the velocity gets faster until the velocity exceeds about $150 \sim 160$ ft sec^{-1}. As discussed before, the linear model deflections are larger than those of the other models.

For stochastic analysis, the power spectrum density of the random process h_R is assumed as the form in eqn (4). Figures 9–12 express the standard deviation of the transverse deflection of the beam, which was attached with the foundation and the profile mean $h_m(x) = \sin 2\pi x/L$ ft, with respect to time for various velocities and accelerations of the train runs. The linear model still has the largest maximum standard deviation of transverse deflection w, however, the range of standard deviation of deflections for model 3 is less

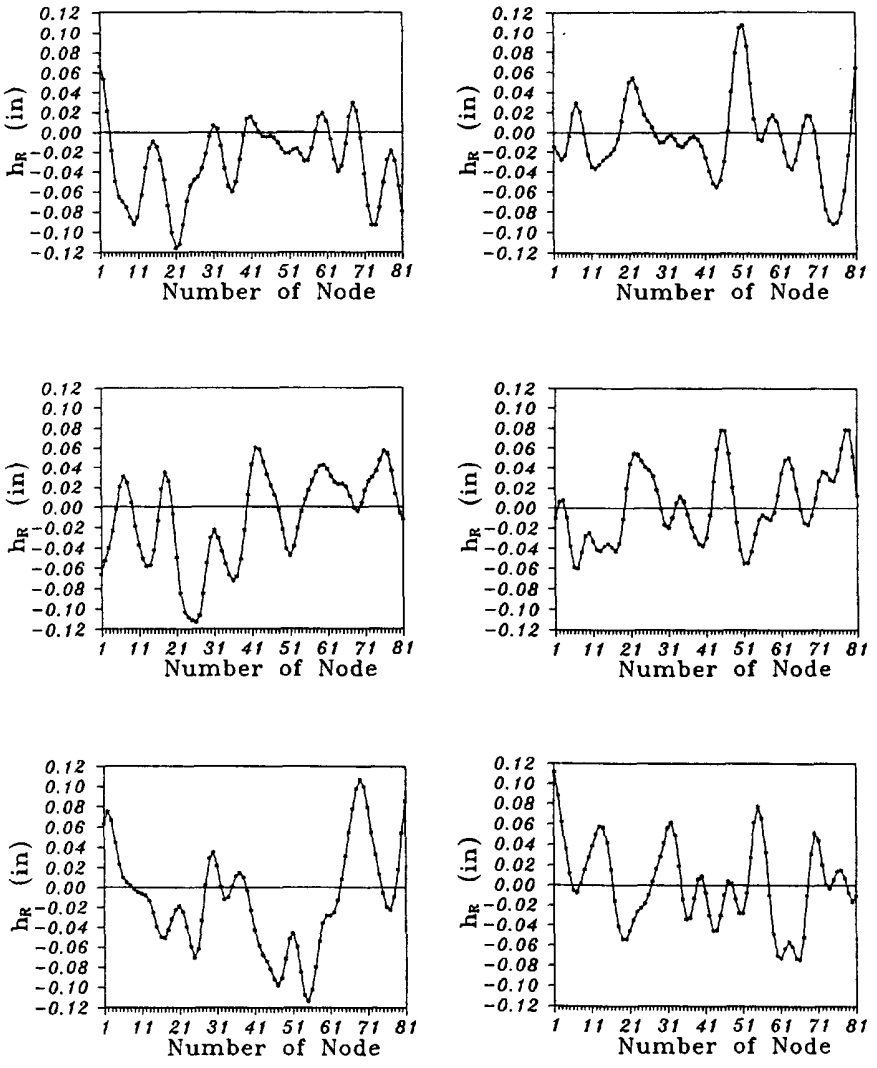

Fig. 3. Six samples of stochastic track profile $h_R(x)$.

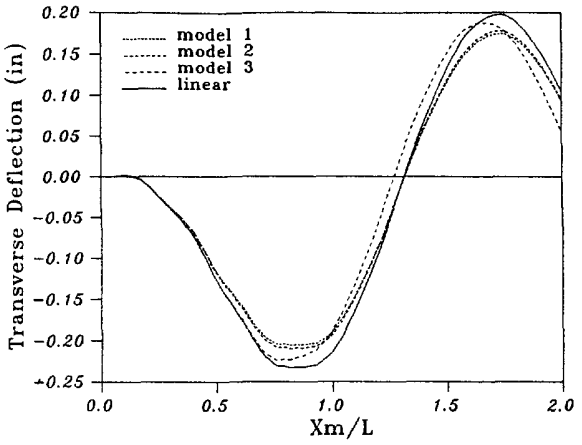

Fig. 4. The midpoint deflection of the beam with foundation, $b = 0$, $b_0 = 0$, $b_1 = 120$ ft sec^{-1}, $b_2 = 0$, $h_m(x) = \sin 2\pi x/L$ ft.

than that of the other three models. Also, it can be seen from Figs 9–12 that among those three nonlinear models, model 2 produced the largest maximum standard deviation of

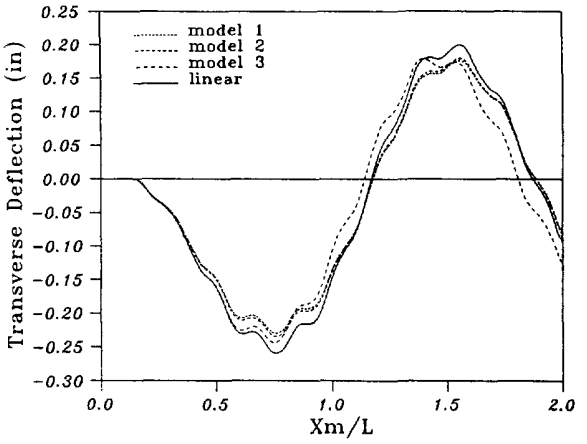

Fig. 5. The midpoint deflection of the beam with foundation, $b = 0$, $b_0 = 0$, $b_1 = 100$ ft sec^{-1}, $b_2 = 0$, $h_m(x) = \sin 2\pi x/L$ ft.

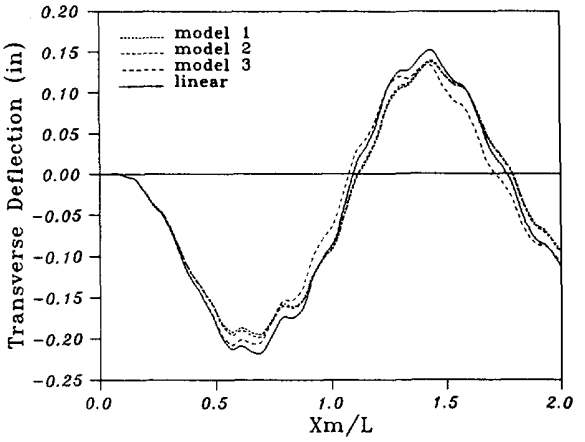

Fig. 6. The midpoint deflection of the beam with foundation, $b = 2$, $b_0 = 0$, $b_1 = 80$ ft sec^{-1}, $b_2 = 10$ ft sec^{-2}, $h_m(x) = \sin 2\pi x/L$ ft.

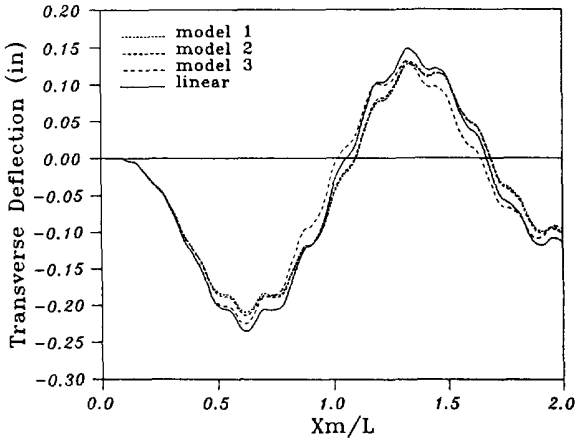

Fig. 7. The midpoint deflection of the beam with foundation, $b = 2$, $b_0 = 0$, $b_1 = 80$ ft sec^{-1}, $b_2 = 5$ ft sec^{-2}, $h_m(x) = \sin 2\pi x/L$ ft.

transverse deflection w, while model 3 produced the smallest maximum standard deviation of transverse deflection w. It is quite interesting that the above results of stochastic analysis are different from those of deterministic analysis.

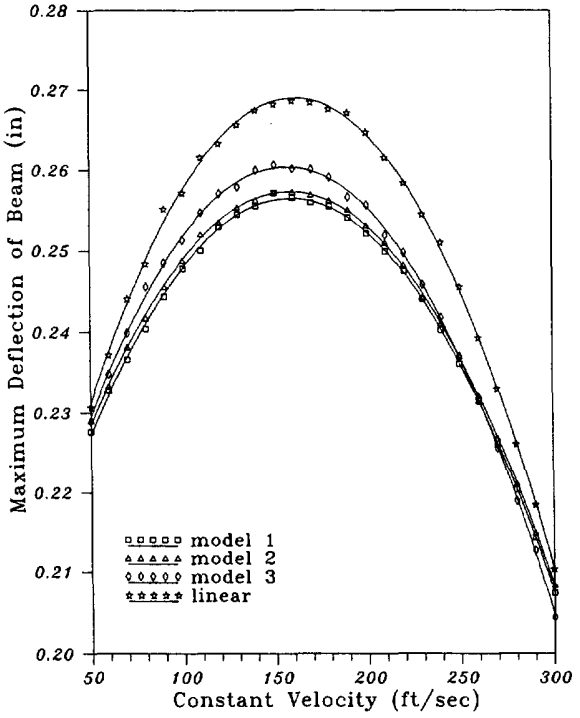

Fig. 8. The maximum deflection of the beam for various constant velocities.

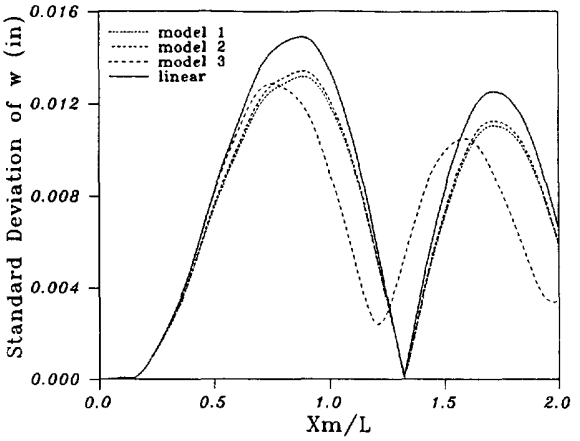

Fig. 9. The standard deviation of the deflection of the beam with foundation, $b = 0, b_0 = 0, b_1 = 120$ ft sec^{-1}, $b_2 = 0$, $h_m(x) = \sin 2\pi x/L$ ft.

To study the distribution of the statistical response, the goodness of fit is tested for some cases such as normal and log normal distribution, by plotting the data on the corresponding probability papers. In Figs 13 and 14, based on Monte Carlo simulation analysis, 100 different values of midpoint deflection of the beam for the time $X_m/L = 0.5$ due to various velocities of the train for model 1 are plotted on the normal probability paper. It can be concluded that the normal distribution fits best for the midpoint deflection of the beam.

6. SUMMARY

In this paper, the nonlinear vibrations of the beam with the foundation due to a general forward velocity of moving load, which can simulate the moving of trains or airplanes, have been analyzed by using the Galerkin's method in conjunction with the finite element

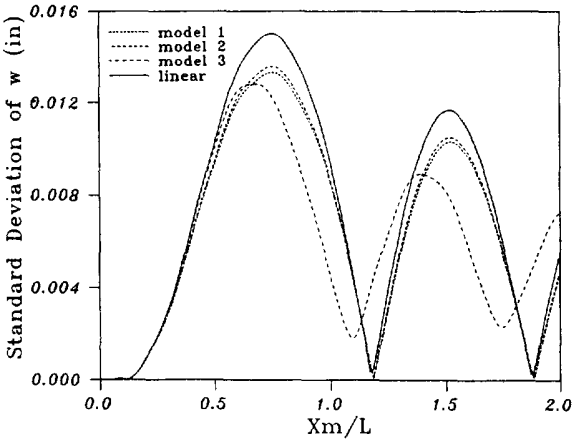

Fig. 10. The standard deviation of the deflection of the beam with foundation, $b = 0$, $b_0 = 0$, $b_1 = 100$ ft sec^{-1}, $b_2 = 0$, $h_m(x) = \sin 2\pi x/L$ ft.

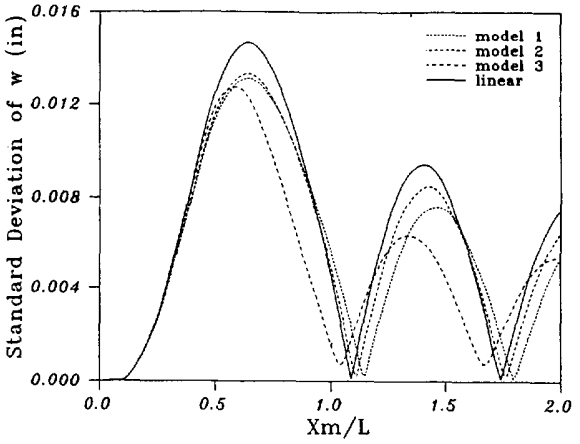

Fig. 11. The standard deviation of the deflection of the beam with foundation, $b = 2$, $b_0 = 0$, $b_1 = 80$ ft sec^{-1}, $b_2 = 10$ ft sec^{-2}, $h_m(x) = \sin 2\pi x/L$ ft.

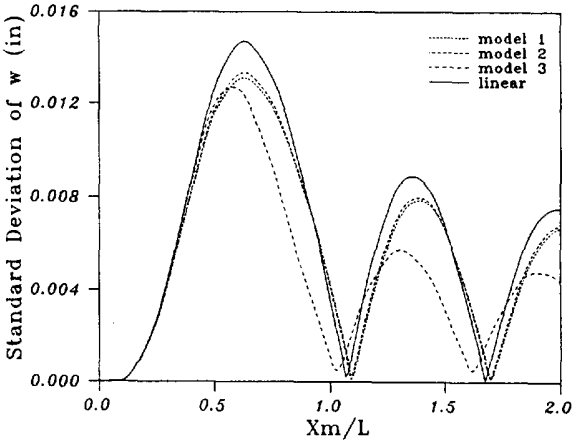

Fig. 12. The standard deviation of the deflection of the beam with foundation, $b = 2$, $b_0 = 0$, $b_1 = 80$ ft sec^{-1}, $b_2 = 5$ ft sec^{-2}, $h_m(x) = \sin 2\pi x/L$ ft.

method. The derived nonlinear equations were linearized by using the incremental method, and the transitional responses computed by the Newmark method. The responses at mid-point of the beam for model 1 always have the smallest amplitudes as compared with those for the other three models. The linear model, however, has the largest amplitude. The speed

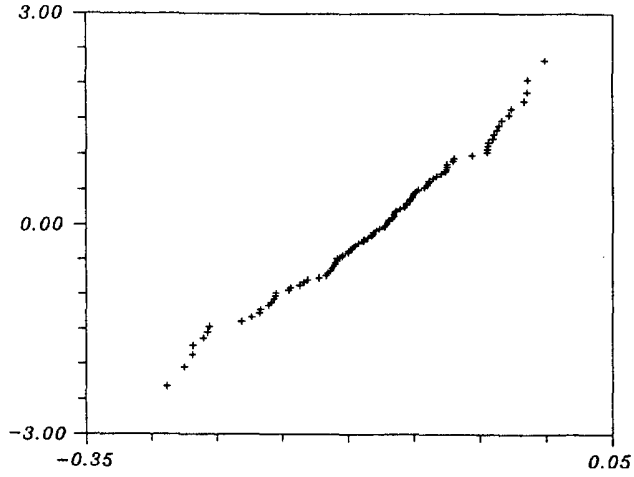

Fig. 13. One-hundred values for the midpoint deflection of the beam for model 1 plotted on the normal probability paper, $b = 0$, $b_0 = 0$, $b_1 = 120$ ft sec^{-1}, $b_2 = 0$, $h_m(x) = \sin 2\pi x/L$ ft.

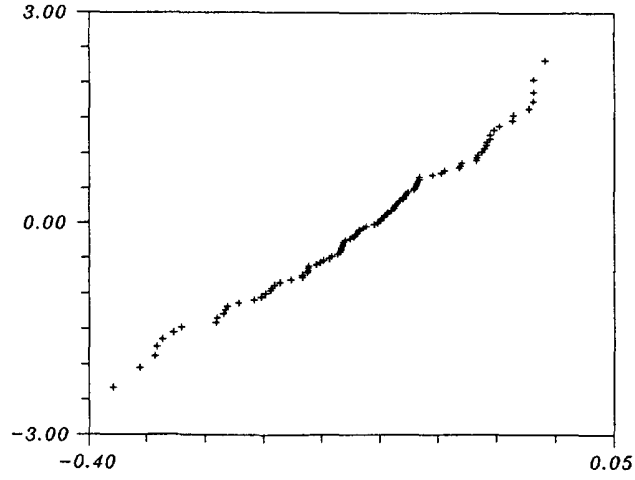

Fig. 14. One-hundred values for the midpoint deflection of the beam for model 1 plotted on the normal probability paper, $b = 0$, $b_0 = 0$, $b_1 = 100$ ft sec^{-1}, $b_2 = 0$, $h_m(x) = \sin 2\pi x/L$ ft.

of the train also has an important influence on the deflection of the beam. The faster the speed of the train, the larger maximum deflection until the velocity exceeds about 150 ~ 160 ft sec^{-1}.

In order to have common discussions, the beam is superimposed by a zero mean random roughness. The Monte Carlo simulation method is then used to perform the statistical dynamic analysis of the stochastic beam on the elastic foundation due to the complicated nature of the present problem. As discussed in the previous paragraph, the standard deviation of the midpoint deflection of the beam for the linear model is always the largest among those of the four models. Also, the distribution of the midpoint deflection when the time for the train located at the midpoint of the beam, i.e. $X_m = L/2$, is normal since the distribution function is represented by a straight line on the normal probability paper.

In future study, the stiffness of the track or the nature of the foundation can be assumed randomly along the position. Besides, the cross-section of the track can be considered as non-uniform.

Acknowledgement—This work was partially supported by the National Science Council of the Republic of China under grant 83-0401-E005-001. The authors are grateful for this support.

REFERENCES

Bathe, K. J., Bolourchi, S., Ramaswamy, S. and Snyder, M. D. (1978). Some computational capabilities for nonlinear finite element analysis. *Nuclear Engng Design* **46,** 429–455.

Bathe, K. J., Ramm, E. and Wilson, E. L. (1975). Finite element formulations for large deflection dynamic analysis. *Int. J. Numer. Meths Engng* **9,** 353.

Bhashyam, G. R. and Prathap, G. (1980). Galerkin finite element method for non-linear beam vibrations. *J. Sound Vibration* **72,** 191.

Criner, H. E., McCann, G. D., Pasadena and Calif (1953). Rails on elastic foundations under the influence of high-speed travelling loads. *J. Appl. Mech.* **20,** 13.

Dodd, C. J. and Robson, J. D. (1973). The description of road surface roughness. *J. Sound Vibration* **31,** 175.

Fryba, L. (1976). Non-stationary response of a beam subject to a moving random force. *J. Sound Vibration* **46,** 323–338.

Hino, J., Yoshimura, T. and Ananthanarayana, N. (1985). Vibration analysis of non-linear beams subjected to moving loads using the finite element method. *J. Sound Vibration* **100,** 477–491.

Hino, J., Yoshimura, T., Konishi, K. and Ananthanarayana, N. (1984). A finite element method prediction of the vibration of a bridge subjected to a moving vehicle load. *J. Sound Vibration* **96,** 45–53.

Kerr, A. D. (1972). The continuously supported rail subjected to an axial force and a moving load *Int. J. Mech. Sci.* **14,** 71.

Mei, C. (1972). Nonlinear vibration of beams by matrix displacement method. *Am. Inst. Aeronautics Astronautics J.* **10,** 355–357.

Nickell, R. E. (1976). Nonlinear dynamics by mode superposition. *Comp. Meths in Applied Mechs Engng* **7,** 107–129.

Prathap, G. and Bhashyam, G. R. (1980). Comments on nonlinear vibrations of immovably supported beams by finite-element method. *Am. Inst. Aeronautics Astronautics J.* **18,** 733–734.

Rades, M. (1972). Dynamic analysis of an inertial foundation model. *Int. J. Solids Structures* **8,** 1353.

Raju, K. K., Shastry, B. P. and Rao, G. V. (1976). A finite element formulation for the large amplitude vibrations of tapered beams. *J. Sound Vibration* **47,** 595–598.

Raju, L. S., Rao, G. V. and Raju, K. K. (1976). Large amplitude free vibrations of tapered beams. *Am. Inst. Aeronautics Astronautics J.* **14,** 280–282.

Sato, H. (1980). Non-linear free vibrations of stepped thickness beams. *J. Sound Vibration* **72,** 415–422.

Suzuki, S. J. (1977). Dynamic behaviour of a finite beam subjected to travelling loads with acceleration. *J. Sound Vibration* **55,** 65–70.

Yoshimura, T., Hino, J., Kamata, T. and Ananthanarayana, N. (1988). Random vibration of a non-linear beam subjected to a moving load by a finite element analysis. *J. Sound Vibration* **122,** 317–329.